Published in final edited form as:
Science. 2010 November 19; 330(6007): 1113–1116. doi:10.1126/science.1194869.

Universality in the Evolution of Orientation Columns in the Visual Cortex

Matthias Kaschube[1,2,*], **Michael Schnabel**[1,3], **Siegrid Löwel**[4,5,6], **David M. Coppola**[7], **Leonard E. White**[8], and **Fred Wolf**[1,5,*]

[1]Max-Planck-Institute for Dynamics and Self-Organization, Bernstein Center for Computational Neuroscience, Faculty of Physics, Göttingen University, D-37073 Göttingen, Germany; and Kavli Institute for Theoretical Physics, Santa Barbara, CA 93106-4030, USA

[2]Lewis-Sigler Institute for Integrative Genomics, Department of Physics, Princeton University, Princeton, NJ 08544, USA

[3]Physical Sciences–Oncology Center, Northwestern Institute on Complex Systems, Departments of Applied Mathematics and Physics, Northwestern University, Evanston, IL 60208, USA

[4]Institute for General Zoology and Animal Physiology, University of Jena, D-07743 Jena, Germany

[5]Bernstein Focus for Neurotechnology, Göttingen University, D-37073 Göttingen, Germany

[6]School of Biology, Göttingen University, D-37073 Göttingen, Germany

[7]Department of Biology, Randolph-Macon College, Ashland, VA 23005, USA

[8]Department of Community and Family Medicine, Duke Institute for Brain Sciences, Duke University, Durham, NC 27710, USA

Abstract

The brain's visual cortex processes information concerning form, pattern, and motion within functional maps that reflect the layout of neuronal circuits. We analyzed functional maps of orientation preference in the ferret, tree shrew, and galago—three species separated since the basal radiation of placental mammals more than 65 million years ago—and found a common organizing principle. A symmetry-based class of models for the self-organization of cortical networks predicts all essential features of the layout of these neuronal circuits, but only if suppressive long-range interactions dominate development. We show mathematically that orientation-selective long-range connectivity can mediate the required interactions. Our results suggest that self-organization has canalized the evolution of the neuronal circuitry underlying orientation preference maps into a single common design.

In the visual cortex of carnivores and primates, neurons selective for the orientation of visual edges are organized in orientation columns, which are vertical arrays of neurons that prefer the same orientation (1–5). Not all mammals have orientation columns (4). Mammalian taxa

*To whom correspondence should be addressed. kaschube@princeton.edu (M.K.); fred-wl@nld.ds.mpg.de (F.W.).

Supporting Online Material
www.sciencemag.org/cgi/content/full/science.1194869/DC1
Materials and Methods
SOM Text
Figs. S1 to S24
Tables S1 to S5
References

that do have been on separate evolutionary paths for more than 65 million years (Fig. 1A) (6–8), colonizing disparate ecological niches and evolving disparate cortical architectures (9). Nevertheless, these taxa share an architecture of orientation columns arranged around numerous singularities, called pinwheel centers (2, 3, 5, 10, 11). Around each singularity, the neuronal preferences for stimulus orientation are circularly arranged, ascending, in a spiral staircase, either clockwise or counter-clockwise from 0° to 180°. Pinwheel organization is similar across disparate mammalian taxa; it is, however, unknown whether this qualitative similarity is imposed by evolutionary history, ecological or developmental constraints, or neural function. To address these issues, we analyzed the arrangement of pinwheels in the visual cortex of three phylogenetically and ecologically diverse species (6–8, 12): the tree shrew(*Tupaia belangeri*), galago (*Otolemur crassicaudatus*), and ferret (*Mustela putorius*). Tree shrews and galagos are more closely related to rodents and lagomorphs, which lack orientation columns (4, 9), than to carnivores (6–8). This taxonomic sample allowed us to compare mammals diverging from the primate lineage either before (ferrets) or after (tree shrews) the supraprimate ancestor (Fig. 1A).

We developed a statistical approach based on the concept of pinwheel density ρ (13), which we define as the mean number of pinwheels per orientation-hypercolumn area (1). For geometrically defined subregions of each map, we calculated independent estimates of local column spacing Λ (14) and pinwheel number, defined the area of an orientation hypercolumn as Λ^2 (14), and estimated the pinwheel density ρ in each sub-region (12). This definition does not presuppose the existence of a discrete set of orientation hyper-columns and is consistent with the original notion (1, 13). Pinwheel density characterizes the layout of orientation columns independently of their absolute size and can differentiate between different column layouts (Fig. 1B) (13, 15–17) that may occur even in directly adjacent cortical regions (Fig. 1, C and D).

We first examined the mean pinwheel density averaged over entire hemispheres. Whereas hyper-column sizes varied substantially between individuals and species, the number of pinwheels occurring per square millimeter scaled with hypercolumn size so that the average pinwheel density was virtually identical (Fig. 2,Aand B): 3.12 [3.06, 3.18] {mean [2.5, 97.5] percentiles of bootstrap confidence interval (BCI) (fig. S7) (12) in tree shrew, 3.15 [2.97, 3.30] in galago, and 3.15 [3.08, 3.22] in ferret (values were confirmed with automated analysis) (fig. S4) (12)}.

Second, we assessed intramap heterogeneity and local arrangement of neighboring pinwheels. We characterized the variability of pinwheel densities by its standard deviation (SD) in subregions of size A between one and 30 hypercolumns (Fig. 2, C and D). SDs of pinwheel densities were very similar for tree shrew, galago, and ferret and different from values characterizing a distribution of randomly positioned pinwheels (fig. S6) (12). Analyzing histograms of nearest-neighbor (NN) distances in units of local column spacing of the respective cortical region for the three species, we observed virtually identical distributions (Fig. 2E). Histograms were also similar when calculated for pairs of same or opposite topological charges (Fig. 2F), where charge denotes whether preferred orientations increase clockwise or anti-clockwise around a pinwheel center (Fig. 1F).

These observations suggest that orientation column layouts follow a common design characterized by the virtual identity of (i) pinwheel density, (ii) pinwheel density fluctuations as a function of subregion size, and (iii) NN distance distributions. An objective quantitative assessment of pinwheel density and its fluctuations and of the NN distance statistics confirmed this concept. To quantitatively compare pinwheel density fluctuations, we defined a variability exponent, γ, and a variability coefficient, c, and estimated them by fitting the SD(A) curves with $c(\rho/A)^{\gamma}$ (figs. S6, S10) (12), where A is the subregion size. To assess the similarity of the NN distance statistics, we used the average distances of NN pinwheels, d, and of pinwheels of same or opposite topological charges, d^{++} and d^{+-} (fig. S11) (12). Relative differences in all parameters were on average below 9%, with one exception below 5% (tables S1 and S2) (12). Furthermore, almost all confidence intervals for the considered parameters overlapped for different species (fig. S7) (12). Thus, in quantitative terms, differences between species were typically very small, confirming the concept of a common design for the layout of orientation columns.

How can this common design observed among species long-separated in mammalian evolution be explained? Recognizing that ancestral eutheria were small-brained nocturnal mammals, with modest visual abilities and a small neocortex that was already subdivided into several cortical areas (6), and that orientation hypercolumns in extant species are relatively large, it is unlikely that orientation columns and the common design are retained from stem eutheria (12). The phylogenetic relations depicted in Fig. lA would then indicate that systems of orientation columns evolved independently in laurasiatheria (such as carnivores) and in euarchonta (such as tree shrews and primates). Alternatively, one might hypothesize that ancestral mammals in the cretaceous already possessed a primitive system of few or miniaturized orientation columns. Even assuming such a homology scenario, the precision with which orientation column layout follows the common design in disparate mammalian lineages implicates a common, constraining developmental mechanism (12).

As the formation and maintenance of orientation-preference maps is activity-dependent (18), we thus examined orientation maps generated by models involving activity-dependent self-organization. In many models, maps reminiscent of the common design transiently appeared but—in agreement with previous reports—subsequently broke down either by pinwheel annihilation producing pinwheel sparse maps (12, 13, 16, 17) or by crystallization of pinwheels into a regular lattice (12, 16, 19, 20). However, in a model in which pinwheels are stabilized through long-range neuronal interactions (12, 17, 21) we found that theoretically predicted maps exhibited all essential features of the common design in a dynamically stable and robust fashion (Figs. 1B, quasi-periodic map, and 3) (12). In this long-range interaction model, only orientation preference and selectivity are mathematically specified for simplicity. Patterns of orientation columns of a given spatial wavelength Λ develop with an effective growth rate r. Whether long-range or short-range interactions stabilize the orientation map is determined by an effective coupling parameter, g (17). Long-range interactions dominate for $\sigma > \Lambda$ and $g < 1$. As we show in (12), this model can be derived from biologically plausible assumptions about the structure of long-range connectivity in the visual cortex.

The mathematical properties of the long-range interaction model suggest an explanation for the emergence of the common design in disparate evolutionary branches (laurasiatherian and euarchontan). Near the instability threshold ($r \ll 1$), a large set of stationary solutions of this model exhibit the property of universality; they are the common solutions of an entire class of models. This class is defined by four symmetry principles that guarantee that maps that are translated or rotated across the cortical surface or for which receptive fields are rotated by a fixed angle can occur with equal probability and that all orientations are represented by the visual cortex (17). Pinwheel configurations in these universal solutions exhibit universal pinwheel statistics, and when the interaction range is substantially larger than one column spacing, these statistics are very similar to the common design (Fig. 3, C and E to H) (12). In fact, apart from a slightly smaller variability coefficient c average differences between pinwheel statistics in representative maps (eq. S20, $n = 20$ active modes) (12) and in experimental observations were below 5% (tables S1 and S2) (12). It is thus not required that exactly the same mechanisms underly map development in disparate lineages as long as they are described by models from the same universality class as the long-range interaction model. Our analyses suggest that such mechanisms of network development include suppressive long-range interactions (12) that extend beyond a single hypercolumn (12) and stabilize the orientation map (12, 15). In numerical simulations of the long-range interaction model, we found that realistic pinwheel statistics can already occur in transient states and farther away from the instability threshold and for interaction ranges between one and two hypercolumns (Fig. 3D) (12). These results suggest that the robust emergence of the common design in mammalian evolution is explained by selection for self-organizing cortical networks dominated by long-range interactions.

To assess this apparent robustness experimentally, we analyzed properties of orientation maps in ferrets reared in darkness beginning about 1 week before eye opening and the emergence of orientation maps (22). Dark-rearing alters the spatiotemporal pattern of activity in the afferent visual pathway, induces abnormal receptive field properties in the lateral geniculate nucleus (23) and visual cortex (24), but does not prevent the formation of orientation maps (Fig. 4, A and B) (22). The average pinwheel density in dark-reared ferrets was 3.22 [3.13, 3.30] and thus indistinguishable from normal ferrets ($P = 0.14$) (Fig. 4C and table S3) (12). Moreover, both pinwheel-density variability and NN distances in dark-reared ferrets were similar to those of normal ferrets, with overlapping confidence intervals for all assessed statistics (12).

For large interaction ranges, the mean pinwheel density predicted by the universal pinwheel statistics rapidly approaches an asymptotic constant equal to π (21). This raises the possibility that the pinwheel density in the common design is a mathematical constant. In support of this possibility, the grand average pinwheel density 3.14 [3.08, 3.20] in all three species was statistically indistinguishable from π. To assess whether our analysis methods might bias mean pinwheel densities toward π, we analyzed randomly generated orientation maps (13) by randomizing the phases of the original measurements in the Fourier domain and then subjected the randomized maps to the same pre-processing and analyses as the original data (Fig. 4, D and E). Randomized maps exhibited significantly higher pinwheel densities {between 3.15 and 3.9, mean = 3.50 [3.41, 3.59]} than what we found in any of the species ($P < 10^{-4}$) (Fig. 4F and tables S1 and S3) (12). For several other statistics, randomized maps differed considerably more from the three analyzed species than the species did from one another (tables S1 to S3) (12).

Our empirical results and theoretical analyses suggest that the precise spatial organization of pinwheels in the visual cortex reflects cortical network self-organization rather than genetic prespecification or environmental instruction of neuronal circuit development. Our theory reveals that dynamical network self-organization can robustly constrain the spatial organization of cortical circuitry to a specific design. Currently, only one alternative arrangement has been observed in nature: the columnless, apparently random, salt-and-pepper organization of rodent visual cortex (4, 9). Because a complete lack of local order appears to be its key feature, we expect that fundamental properties of local rather than long-range circuit formation are essential for its self-organization. It is possible that this fundamentally different organization can also be derived from a dynamical theory of network self-organization. If so, the principles of network self-organization operating on a local order would account for the presence or absence of orientation columns, whereas long-ranging interactions would explain the organization of orientation columns into pinwheels, with a spatial layout conforming to the common design.

Our analysis of the long-range interaction model predicts that spatial range and an overall suppressive nature of nonlocal interactions are essential for the formation of the pinwheel layout in carnivores and primates. These requirements are consistent with the physiological action of nonlocal influences in the visual cortex (12, 25) but hard to reconcile with the notion that pinwheels are quasi-isolated local circuit elements. The relevant genes controlling their formation are thus expected to concern the regulation of lateral axon outgrowth and the setting of overall synaptic input balance (14, 25). Genetic or experimental perturbations that restrict neuronal interactions in the visual cortex to the range of an individual hypercolumn are predicted to induce the breakdown of spatially complex orientation maps into pinwheel sparse or crystal-like patterns. Verification of this prediction would confirm that building cortical networks by self-organization imposes discrete design alternatives. Evolutionary selective pressure could then only drive a switching between discrete circuit types but could not gradually transform one into the other.

Already in 1942, Waddington (26) suggested that robustness of developmental processes may play an adaptive role in evolution, protecting developing organisms from both genetic and environmental perturbations by canalizing the physiological and anatomical organization of organisms into a much narrower range than might be expected from their genetic diversity (27–29). If our explanation of the common design is correct, its evolution represents a genuine example of such canalization through an emergent property of complex cortical networks expressed in long-separated mammalian line-ages. We conclude that wherever such complex biological systems unfold, especially in the mammalian brain where they are likely to abound, the principles of dynamical network self-organization may design and constrain system behavior as powerfully as an organism's genetic endowment or early life experiences.

Supplementary Material

Refer to Web version on PubMed Central for supplementary material.

Acknowledgments

We thank J. Crowley, J. Fischer, T. Geisel, H. Greenside, A. Grinvald, M. Gutnick, J. Kaas, T. Kottos, T. Moser, and J. Schmitz for discussions; B. Bosking for acquiring and processing imaging data; W. Keil and L. Reichl for calculations; B. Goetze for graphics; D. Fitzpatrick for support of imaging experiments (NIH/National Eye Institute (NEI) EY06821 and EY11488); and the Kavli Institute for Theoretical Physics for its hospitality. This work was funded by grants from the Human Frontier Science Program and Bundesministerium für Bildung, Wissenschaft, Forschung und Technologie to S.L. and F.W. (01GQ0430 and 01GQ0922); NSF to D.M.C. (0641433); NIH/ National Institute of General Medical Sciences to M.K. (P50 GM071508); and the Whitehall Foundation to L.E.W. and was supported in part by the National Science Foundation (NSF PHY05-51164).

References and Notes

1. Hubel DH, Wiesel TN. Proc. R. Soc. London Ser. B Biol. Sci. 1977; 198:1. [PubMed: 20635]
2. Blasdel GG, Salama G. Nature. 1986; 321:579. [PubMed: 3713842]
3. Bonhoeffer T, Grinvald A. Nature. 1991; 353:429. [PubMed: 1896085]
4. Ohki K, Chung S, Ch'ng YH, Kara P, Reid RC. Nature. 2005; 433:597. [PubMed: 15660108]
5. Ohki K, et al. Nature. 2006; 442:925. [PubMed: 16906137]
6. Kaas JH. Brain Res. Bull. 2008; 75:384. [PubMed: 18331903]
7. Kriegs JO, et al. PLoS Biol. 2006; 4:e91. [PubMed: 16515367]
8. Kriegs JO, et al. Trends Genet. 2007; 24:156.
9. Van Hooser SD. Neuroscientist. 2007; 13:639. [PubMed: 17911223]
10. Obermayer K, Blasdel GG. Neural Comput. 1997; 9:555. [PubMed: 9097474]
11. Bosking WH, Zhang Y, Schofield B, Fitzpatrick D. J. Neurosci. 1997; 17:2112. [PubMed: 9045738]
12. Materials and methods are available as supporting material on *Science* Online.
13. Wolf F, Geisel T. Nature. 1998; 395:73. [PubMed: 9738500]
14. Kaschube M, Wolf F, Geisel T, Löwel S. J. Neurosci. 2002; 22:7206. [PubMed: 12177215]

15. Durbin R, Mitchison G. Nature. 1990; 343:644. [PubMed: 2304536]
16. Lee HY, Yahyanejad M, Kardar M. Proc. Natl. Acad. Sci. U.S.A. 2003; 100:16036. [PubMed: 14673111]
17. Wolf F. Phys. Rev. Lett. 2005; 95:208701. [PubMed: 16384113]
18. White LE, Fitzpatrick D. Neuron. 2007; 56:327. [PubMed: 17964249]
19. Mayer N, Herrmann JM, Geisel T. Neurocomputing. 2002; 44–46:533.
20. Reichl L, Löwel S, Wolf F. Phys. Rev. Lett. 2009; 102:208101. [PubMed: 19519077]
21. Kaschube M, Schnabel M, Wolf F. N. J. Phys. 2008; 10:015009.
22. White LE, Coppola DM, Fitzpatrick D. Nature. 2001; 411:1049. [PubMed: 11429605]
23. Akerman CJ, Smyth D, Thompson ID. Neuron. 2002; 36:869. [PubMed: 12467590]
24. Li Y, Fitzpatrick D, White LE. Nat. Neurosci. 2006; 9:676. [PubMed: 16604068]
25. Kaschube M, Schnabel M, Wolf F, Löwel S. Proc. Natl. Acad. Sci. U.S.A. 2009; 106:117205.
26. Waddington CH. Nature. 1942; 150:563.
27. Smith, JMaynard, et al. Q. Rev. Biol. 1985; 60:265.
28. Flatt T. Q. Rev. Biol. 2005; 80:287. [PubMed: 16250465]
29. Niven JE. PLoS Biol. 2005; 2:e19.

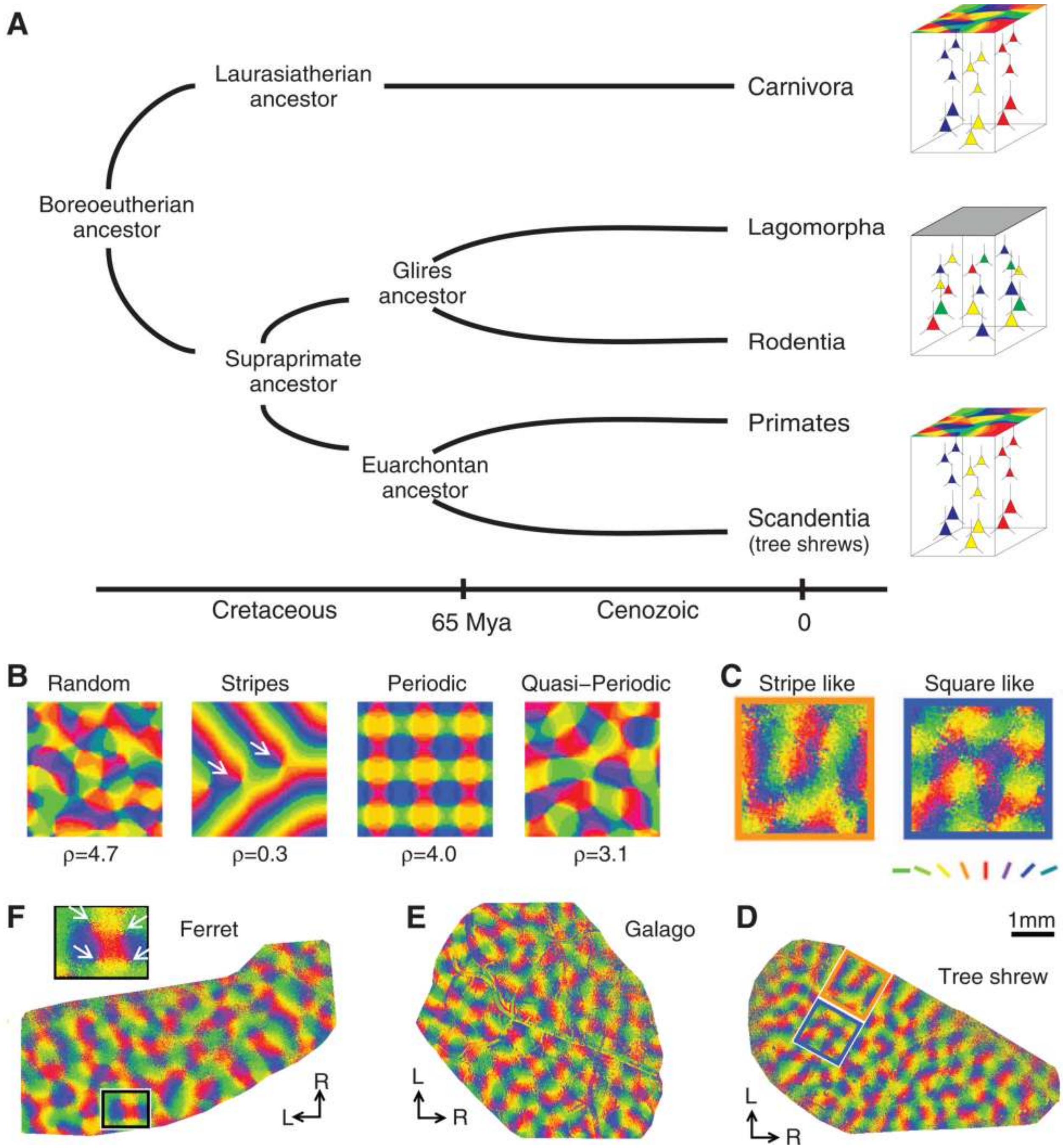

Fig. 1.

Orientation selectivity in the visual cortex of diverse boreoeutherian mammals. (**A**) phylogenetic relationships (6–8) between mammalian ancestors, the three species examined, and rodents and lagomorphs. (Right) Arrangement of orientation-selective neurons in these species. Rodents and lagomorphs show salt-and-pepper arrangement of preferred orientations (ORs). Carnivores, primates, and tree shrews show columnar arrangement of preferred ORs. (**B**) Synthetic orientation maps of equal column spacing Λ but widely different pinwheel densities ρ. From left to right are the solutions of different models (13, 15–17). Colors code preferred ORs as indicated by the bars in (C). (**C**) High (blue frame) and low (orange frame) pinwheel density regions in tree shrew visual cortex. (**D** to **F**)

Optically recorded orientation maps in (D) tree shrew, (E) galago, and (F) ferret visual cortex. Regions shown in (C) are marked in (D).White arrows in (F)mark selected pinwheel centers. Framed regions in (C) and (F) are magnified.

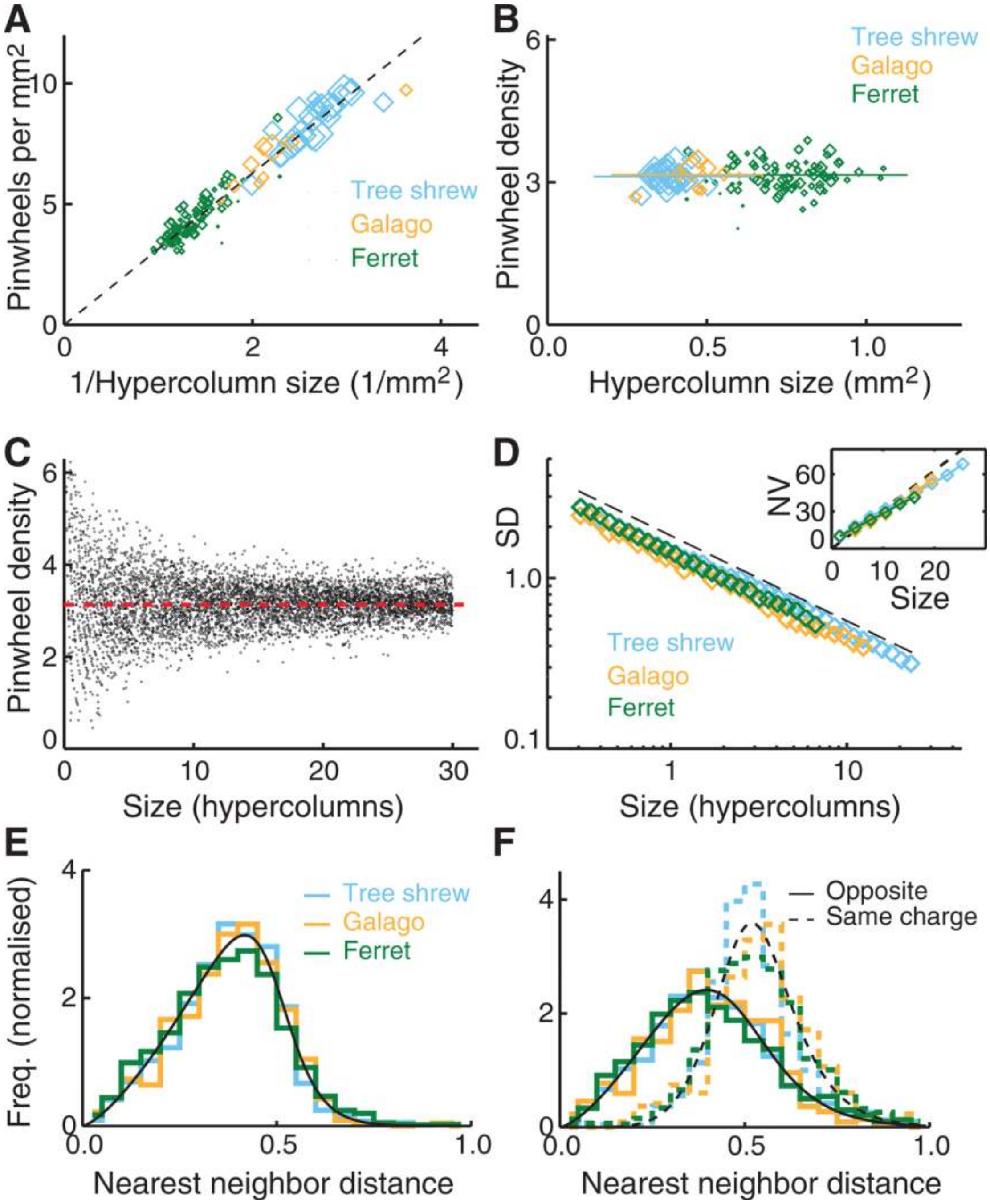

Fig. 2.

Common design of orientation maps and pinwheels in ferret, tree shrew, and galago. (**A**) The mean number of pinwheels per square millimeter, r, scales with the inverse of hypercolumn size Λ^2 in individuals of the three species (tree shrew, *n* = 26 hemispheres; galago, *n* = 9 hemispheres; ferret, *n* = 82 hemispheres; symbol size proportional to map size in units of Λ^2). Dashed line indicates $r = \langle\rho\rangle/\Lambda^2$ (where $\langle\rho\rangle = 3.14$ grand average pinwheel density). (**B**) Dimensionless pinwheel densities ρ versus hypercolumn size. Solid lines indicate average pinwheel densities of the three species. (**C**) Pinwheel densities estimated for regions of up to 30 hypercolumns randomly selected from tree shrew orientation maps (12). Red dashed line indicates average pinwheel density in tree shrew. (**D**) SDs of pinwheel densities estimated from randomly selected regions for the three species. Black dashed curve indicates SD for a two-dimensional Poisson process of equal density. (Inset) Number variance (NV) for tree shrew, ferret, and galago and for the Poisson process. (**E** and **F**) NN distances for pinwheels of (E) arbitrary and (F) opposite and equal topological charge (12). Black curves indicate $f(x) = ax^n/\{1 + \exp[(x - x_0)/b)]\}$ [(E) $n = 1.2$, $x_0 = 0.48$, $b = 0.047$], [(F) solid curve, $n = 1.2$, $x_0 = 0.46$, $b = 0.08$; dashed curve, $n = 4.5$, $x_0 = 0.5$, $b = 0.05$]. Distances are in units of Λ.

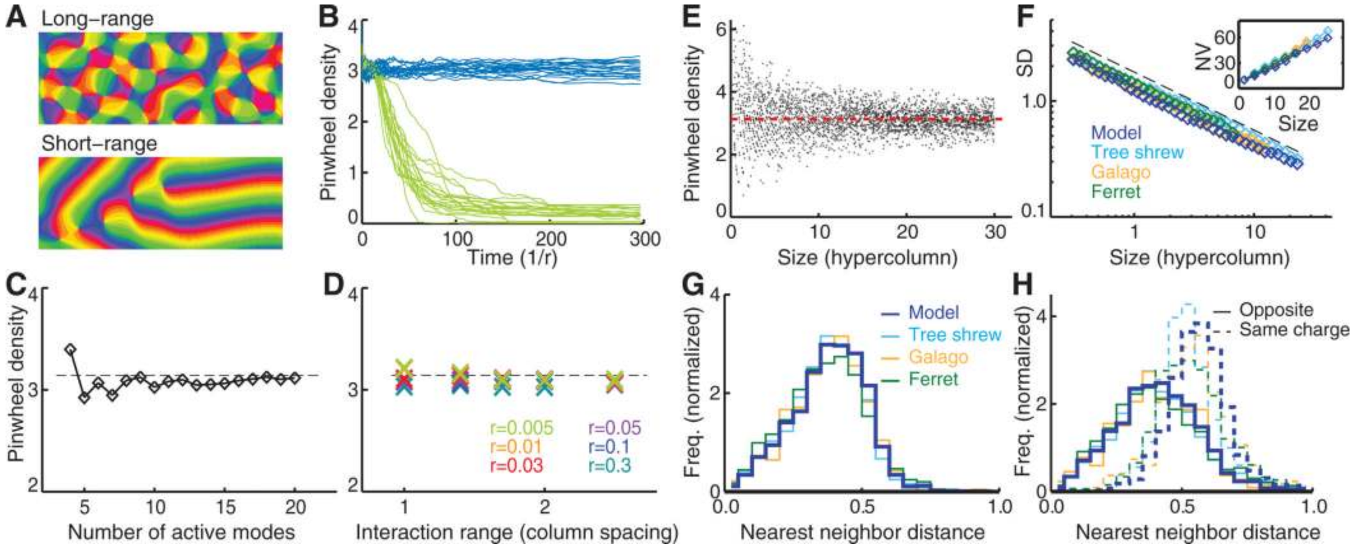

Fig. 3.

Self-organization of orientation columns dominated by long-range interactions explains the common design. (**A**) Nearly stationary solutions of the long-range interaction model (eqs. S10 to S13) (12) are pinwheel-rich when long-range interactions dominate and pinwheel-sparse when they are absent. (**B**) Pinwheel densities as a function of time without long-range interactions (green, $r = 0.1$, $g = 2$, $n = 30$ different random initial conditions) and when long-range interactions dominate (blue, $r = 0.1$, $\sigma = 1.7$, $g = 0.98$, $n = 30$ different random initial conditions). (**C**) Average pinwheel densities $\langle\rho\rangle$ of closed-form solutions for $r \ll 1$ (eq. S20) (12). Solutions consists of n active modes (Fourier components; error bars are smaller than symbol size). In the long-range interaction model, n scales linearly with interaction range σ (12). (**D**) Average densities $\langle\rho\rangle$ in numerical solutions for different r at $t = 300$ ($g = 0.98$, $\sigma = 1.7$). (**E** to **H**) Spatial statistics of pinwheels (as in Fig. 2) for $n = 26$ randomly chosen closed-form solutions (eq. S20, $n = 20$ active modes) (12).

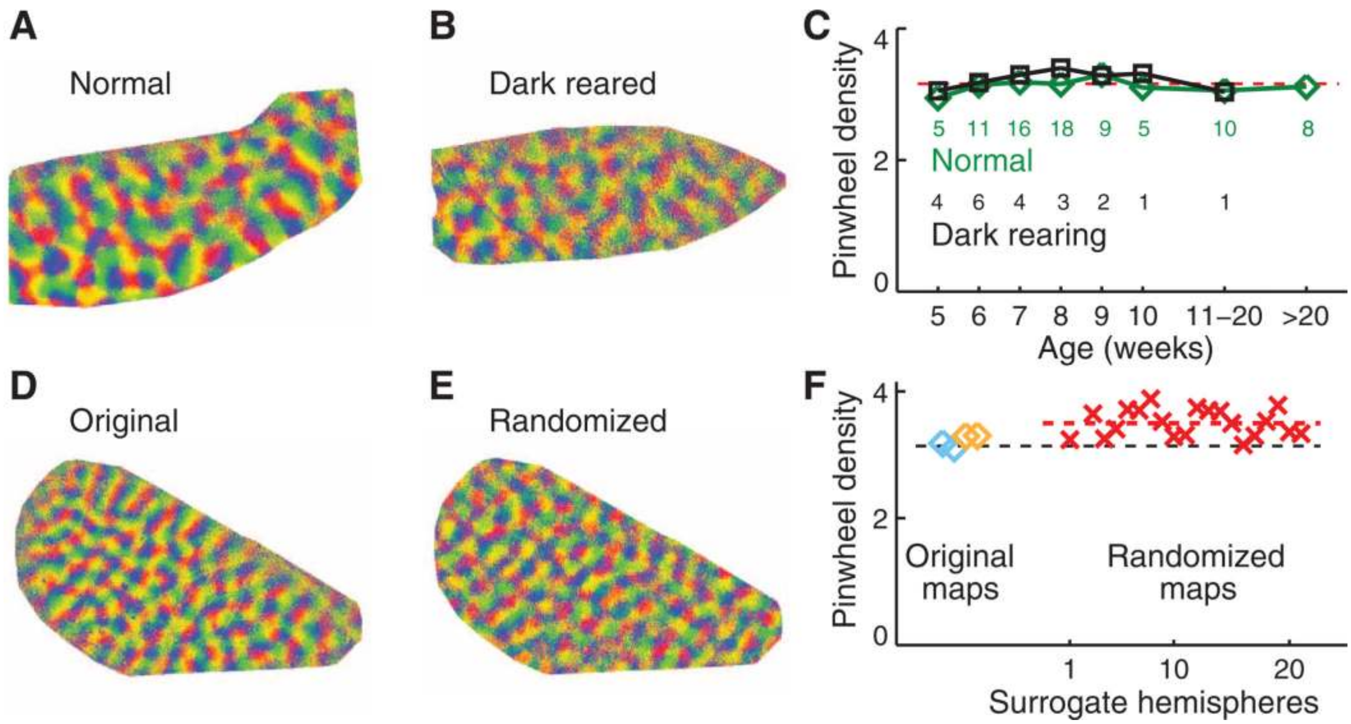

Fig. 4.

The common design persists under dark-rearing (**A** to **C**) but not under phase randomization (**D** to **F**) and is attained early during development (C). Orientation maps from (A) a normal and (B) a dark-reared ferret. (C) Pinwheel densities for dark-reared (n = 21) and normal ferrets (n = 82) versus postnatal age (numbers are the sample sizes). Random orientation maps (E) generated from the tree shrew orientation map (D) by phase shuffling in the Fourier domain (12). (F) Pinwheel densities of randomized maps (crosses, n = 20 randomized maps) and of original maps [diamonds, n = 4 (tree shrew, n = 2; galago, n = 2); five random maps were generated from each original map]. Red dashed line indicates average pinwheel density of randomized maps. Black dashed line indicates 3.14.